LANGMUIR

pubs.acs.org/Langmuir Article

# Structuring Pickering Emulsion Interfaces with Bilayered Coacervates of Cellulose Nanofibers and Hectorite Nanoplatelets

Yeong Sik Cho, Sung Ho Lee, Hye Min Seo, Kyounghee Shin, Min Ho Kang, Minyoung Lee, Jungwon Park, and Jin Woong Kim*

Cite This: *Langmuir* 2021, 37, 3828−3835 Read Online

ACCESS | Metrics & More | Article Recommendations | Supporting Information

**ABSTRACT:** In this study, we present a water-in-silicone oil (W/S) Pickering emulsion system stabilized via in situ interfacial coacervation of attractive hectorite nanoplatelets (AHNPs) and bacterial cellulose nanofibrils (BCNFs). A bilayered coacervate is generated at the W/S interface by employing the controlled electrostatic interaction between the positively charged AHNPs and the negatively charged BCNFs. The W/S interface with the bilayered coacervate shows a significant increase in the interfacial modulus by 2 orders of magnitude than that with the AHNPs only. In addition, we observe that water droplets are interconnected by the BCNF bridging across the continuous phase of silicon, which is attributed to the diffusive transport phenomenon. This droplet interconnection results in the effective prevention of drop coalescence, which is confirmed via emulsion sedimentation kinetics. These results indicate that our bilayered coacervation technology has the potential of developing a promising Pickering emulsion platform that can be used in the pharmaceutical and cosmetic industries.

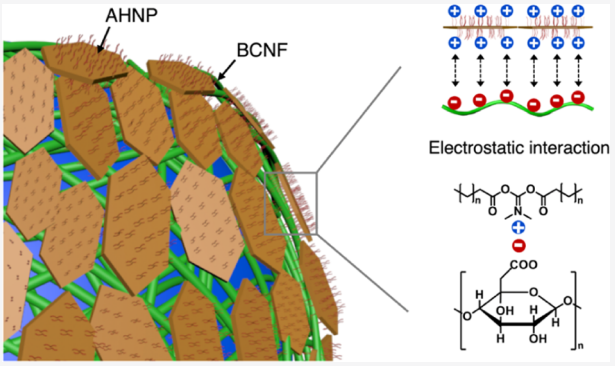


## INTRODUCTION

Clay particles, such as hectorite and laponite, assemble to exhibit a balanced wetting behavior at oil−water (O/W) interfaces,[1−4] which enables the production of Pickering emulsions comprising a mechanically strong solid interface.[5−7] From a geometric point of view, it is interesting to use clay particles with a platelet structure. Owing to the intimately large surface area, they favorably adsorb to the O/W interface once the wettability is well tuned, thus exhibiting excellent barrier performance.[8,9] However, there are inherent interstitial imperfections created because clay particles cannot completely cover the droplets.[10−12] Moreover, electrostatic inter-repulsion between the adsorbed particles impedes the close packing of the particles around the suspended drops.[13,14] Therefore, there have been attempts to cover the interstitial imperfections at the interface of the Pickering emulsions. For instance, denser packing of hectorite nanoplatelets at the water-in-oil (W/O) interface could be achieved by tuning their surface wettability through coating with cationic surfactants.[15−17] In addition, the interstitial distance between clay particles can be reduced by introducing an electrolyte, owing to the electrolyte-induced charge screening effect.[18−20] Furthermore, the interstitial space surrounded by the edges of clay particles can be filled with anionic polymers, thus possibly enhancing the integrity of the interface.[21,22] Nevertheless, since the introduction of such additives cannot significantly prevent the generation of interstitial imperfections at the interface, a more progressive approach to solve this problem is still strongly required.

Herein, we propose a new water-in-silicone (W/S) Pickering emulsion system whose interface is stabilized via interfacial coacervation between anionic bacterial cellulose nanofibrils (BCNFs)[23−26] and cationic attractive hectorite nanoplatelets (AHNPs). In this study, the silicone-dispersible AHNPs and water-dispersible BCNFs electrostatically face each other to form a bilayer structure at the W/S interface. Through this approach, the interstices generated in the AHNP layer can be covered with another layer of BCNFs. The formation of a bilayer consisting of BCNFs and AHNPs was confirmed via direct observation using a confocal laser scanning microscope (CLSM) and a cryo-transmission electron microscope (cryo-TEM). Interfacial rheology analysis was conducted to characterize the interfacial moduli of the bilayered coacervates. The phase separation behaviors of the Pickering emulsions were observed by measuring the sedimentation velocities of the Pickering emulsions and comparing them with the ones obtained theoretically. This study aims to provide a rationale

Received: October 24, 2020
Revised: March 15, 2021
Published: March 29, 2021

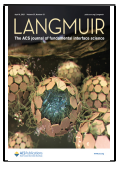







https://doi.org/10.1021/acs.langmuir.0c03082
*Langmuir* 2021, 37, 3828−3835

for the formation of bilayered coacervates at the interface that improve the structural stability of Pickering emulsions.

## EXPERIMENTAL METHODS

**Materials.** Bentone EW was purchased from Elementis (England) and modified into AHNPs.[27] The AHNP coated with a cationic surfactant, dimethyl dihydrogenated tallow ammonium chloride (2M2HT), was supported by Sunjin Beauty Science Co. (Korea). Neat bacterial cellulose (BC) was supplied by SK Bioland (Korea). Cyclopentasiloxane (KF-995) ($M_w \sim 370$) was purchased from Shin-Etsu Silicone Co. (Japan) and used as the continuous phase (kinematic viscosity: 4 $mm^2/s$ at room temperature (RT)). Fluorescein isothiocyanate isomer I (FITC), direct red 23, 2,2,6,6-tetramethylpipridine-1-oxyl radical (TEMPO), sodium bromide, and sodium hypochlorite solution (12%) were purchased from Sigma-Aldrich. Deionized doubled distilled water (DI water) was used in all experiments.

**Suspension of Cationically Charged AHNPs in a Silicone Oil.** To obtain a cationically charged AHNP suspension in a silicone oil, 2M2HT-treated AHNPs were exfoliated by repeatedly high-pressure homogenization. For this, the AHNPs (5 g) were well-dispersed in 250 mL of silicone oil (KF-995) by mechanically stirring at 2000 rpm for 20 min at room temperature. Then, high-pressure homogenization was conducted at 1500 bar with five cycles using a high-pressure homogenizer (MF400BF, Micronox, Korea) at room temperature, which produced a fine AHNP suspension. The AHNP suspension had about 89% yield after five-cycle homogenization and a viscosity of 2100 Pa·s. The AHNP suspension prepared was stored at 4 °C before use.

**Fine Dispersion of Anionically Charged BCNFs in Water.** To provide anionic charges onto the BCNFs, TEMPO-mediated oxidation was carried out for neat BC. BC (1 g) was dispersed in water (300 mL) with TEMPO (0.016 g, 0.1 mmol) and sodium bromide (0.1 g, 1 mmol) until no suspended solids were observed. Next, a NaClO solution (15.08 mg, 10 mmol) was slowly added into the mixture solution. The pH of the suspension was tuned between 10 and 11 by adjusting a NaOH solution (0.5 M). The aqueous suspension of TEMPO-oxidized BCNFs was exhaustively washed with a mixture of ethanol and water (80% v/v). The solid content of BCNFs in water was fixed with 0.33 wt %. The BCNF suspension was stored at 4 °C before use.

**Production of W/S Pickering Emulsions by Interfacial Coacervation.** AHNP/BCNF-bilayered W/S Pickering emulsions were produced by using conventional emulsification. First, 10 mL of the AHNP suspension in KF-995 (0.15 w/v) was placed in a beaker and gently stirred at 2000 rpm for 5 min at room temperature. After adding 0.5 wt % BCNFs dropwise in the aqueous suspension (4.5 mL), the mixture was emulsified using a conventional homogenizer (T25 basic, IKA Works, Inc., Germany) at 15 000 rpm for 10 min at room temperature. Any air bubbles in the emulsion were removed by degasification, in which decompression of 0.1 mPa is applied to the on-prepared emulsion. To investigate how the ratio of water and silicone oil affects the type of emulsions (W/S or S/W), a series of Pickering emulsions were prepared with varying ratios from 1:9 to 9:1 (v/v) in the presence of 0.15 wt % AHNPs in oil and 0.5 wt % BCNFs in water.

**Characterizations.** To confirm the formation of a bilayered coacervate at the interface of Pickering emulsion drops, AHNPs were tagged with FITC and BCNF with direct red 23, and then each layer was visualized using a confocal laser scanning microscope (CLSM, LSM710, Carl Zeiss, Germany). The W/S Pickering emulsions prepared in this study were observed with a bright-field microscope (Axio Vert. A1, Carl Zeiss, Germany). The sedimentation kinetics of emulsions was examined by monitoring the emulsion phase change in a glass tube at room temperature using a CCD camera (MV-CE060-10UC, Hikvision, China). The interfacial tension between water/silicone oil was analyzed with a tensiometer (DCA-200S, S.E.O, Korea). For cryo-transmission electron microscopy (cryo-TEM) and cryo-high-angle annular dark-field scanning transmission electron microscopy (cryo-HAADF-STEM) observations, 3 $\mu$L of the emulsion was applied to the backside of a glow-discharged 200 mesh carbon film-supported copper grid, blotted for 5 s, and then plunge-frozen in liquid ethane using an FEI Vitrobot TM. The grid was loaded onto a cryo-transfer holder (Model 626, Gatan) and imaged in a JEM-2100F transmission electron microscope (JEOL Ltd., Japan) operated at 200 kV and equipped with an UltraScan 1000XP detector (Gatan) and imaged in a JEM-2100F transmission electron microscope (JEOL Ltd., Japan) operated at 200 kV and equipped with an UltraScan 1000XP detector (Gatan) and imaged in a JEM-2100F transmission electron microscope (JEOL Ltd., Japan) operated at 200 kV and equipped with an UltraScan 1000XP detector (Gatan). Energy-dispersive X-ray spectroscopy was performed using AZtecTEM software.

**Rheological Measurements.** Rheological properties were characterized using a DHR-3 rheometer (TA instrument) in the stress control mode with a cone−plate geometry, the diameter of which was 40 $\mu$m and the angle was 2°. Before measuring all rheological measurements, equilibration was performed for 10 min. Then, a solvent trap wrapped the sample to prevent any other evaporation. The rheology was characterized by the running flow sweep, oscillation amplitude sweep, and time sweep tests. The flow sweep measurement was conducted at shear rates ranging from 0.001 to 100 $s^{-1}$. The strain range of the oscillation amplitude was controlled in the range of 0.01−100%. The frequency amplitude measurement was conducted at a frequency range of 100−0.1 rad/s. All of the experiments were carried out at 25 °C. In the case of measuring interfacial rheology of coacervated membranes, the rheometer was equipped with a Du Noüy ring.

## RESULTS AND DISCUSSION

**Design of Bilayered Coacervation at the W/S Pickering Emulsion Interface.** In a typical interfacial coacervation technique, O/W Pickering emulsions are stabilized by adsorption of preformed coacervates from the aqueous phase onto the oil drops, which eventually strengthens the O/W interface. Because of the specificity of this process, it is mostly applied to the O/W emulsion system. In this study, we aim to show that interfacial coacervation is possible even in a W/O emulsion system using the oppositely charged AHNPs and BCNFs. Therefore, to form an interfacial coacervate through the electrostatic interaction, we designed a W/S emulsion system with a bilayered coacervate structure at the interface, wherein the AHNPs diffuse from the continuous phase of the silicone oil and the BCNFs diffuse from the aqueous dispersion phase to the W/S interface (Figure 1).

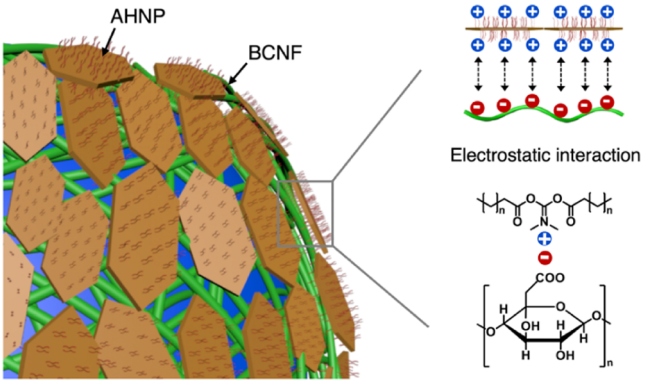


**Figure 1.** Schematic illustration of bilayered interfacial coacervation of the cationic AHNPs and the anionic BCNFs at the W/S Pickering emulsion interface.



https://doi.org/10.1021/acs.langmuir.0c03082
Langmuir 2021, 37, 3828−3835

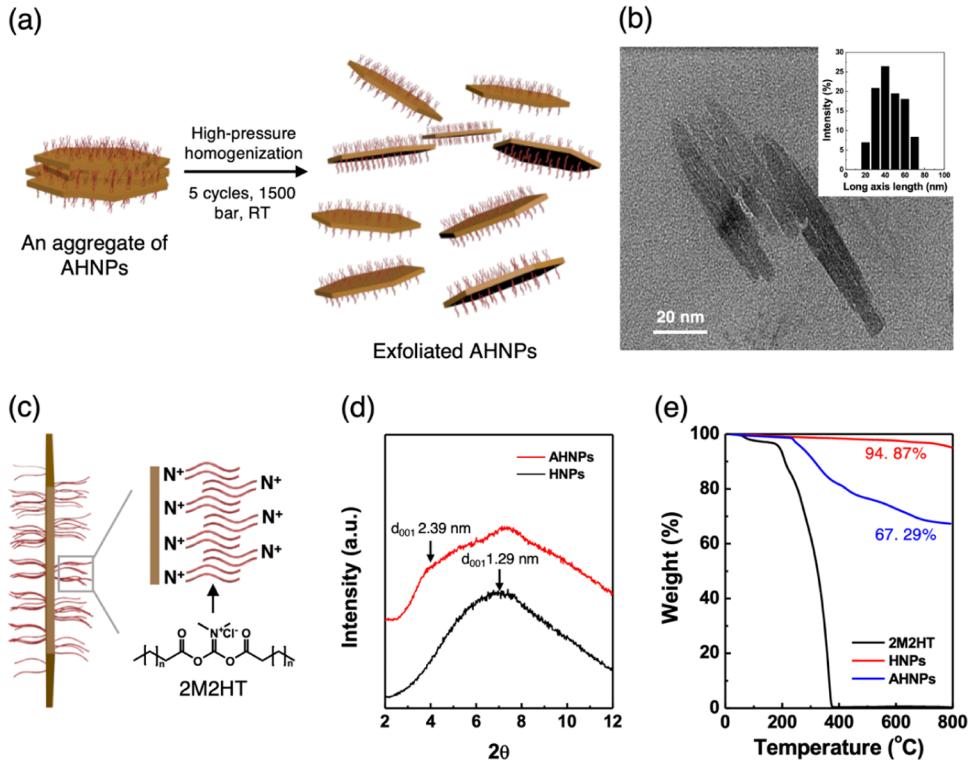


**Figure 2.** (a) Schematic illustration of the fabrication of the exfoliated AHNPs by in situ exfoliation of a microscopic aggregate of AHNPs via high-pressure homogenization. (b) TEM image and size distribution of AHNPs (inset) fabricated through five-cycle high-pressure homogenization. (c) Schematic illustration of modifying the AHNPs' surface with a cationic surfactant, 2M2HT. (d) XRD and (e) TGA analyses of the AHNPs.

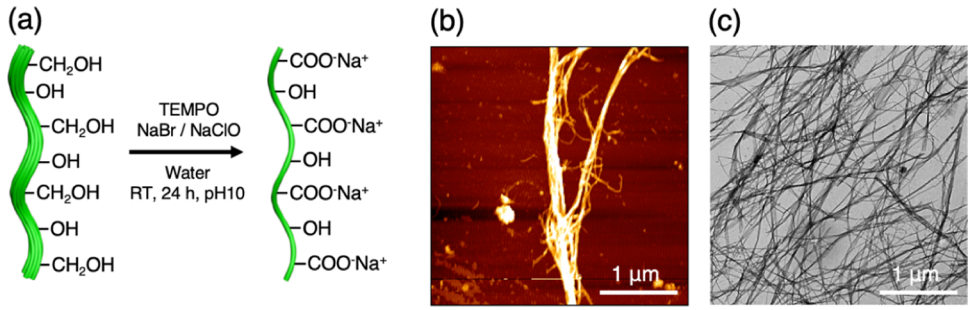


**Figure 3.** (a) Synthesis of BCNFs from a bundle of BCs via TEMPO oxidation. (b) AFM image of the BCNFs. (c) TEM image of the BCNFs.

First, we exfoliated the AHNP aggregates to fabricate a fine dispersion of thin nanoplatelets in the silicone oil through high-pressure homogenization (Figure 2a). Through TEM analysis, we observed that after exfoliation, the average thickness and long axis length of the AHNPs were ∼8 and ∼50 nm, respectively (Figure 2b). The particle size in terms of the long axis length showed a relatively uniform distribution at a size less than 100 nm. Thereafter, we confirmed that the treatment with a cationic surfactant, 2M2HT, provided the surface of AHNPs with positive charges (∼10 mV) (Figure 2c).[28,29] Successful surface modification of the AHNPs with 2M2HT was also confirmed from the X-ray diffraction (XRD) pattern, indicating that the basal spacing ($d_{001}$) of the AHNPs increased from 1.29 to 2.39 nm because of the intercalation of 2M2HT between hectorite layers. (Figure 3d).[30] Through thermogravimetric analysis (TGA), we confirmed that the surface of the AHNPs was coated with approximately 33% of 2M2HT (Figure 2e).[31] Separately, we also fabricated BCNFs via TEMPO-mediated oxidation that allowed us to convert the primary hydroxyl groups on neat BC into carboxylate groups (Figure 3a). The BCNFs having negative charges with −60 mV of $\zeta$-potential readily interact with the AHNPs electrostatically. Atomic force microscopy (AFM) and TEM analyses revealed that the thickness and the length of the BCNFs were approximately 20 nm and 3 $\mu$m, respectively (Figure 3b,c).

**Direct Microscopic Verification of the Formation of Bilayered Interfacial Coacervates.** We first investigated the types of emulsions (W/S or S/W) with varying ratios of water and silicone oil. Our emulsion system showed the typical inversion from the W/S emulsion to the S/W emulsion at around 50 vol % water (Figure S1 and Table S1). For the production of stable W/S emulsions, in this study, the ratio of water and silicone oil was set to 3/7 (v/v). We observed that a stable W/S emulsion could be formed when more than 2 wt % AHNPs were introduced. This is because the AHNPs formed a house-of-card gel structure in the silicone oil phase.[32] However, this effect disappeared at a concentration of 1 wt % or less, and phase separation occurred easily (Figure 4a, also


https://doi.org/10.1021/acs.langmuir.0c03082
Langmuir 2021, 37, 3828−3835

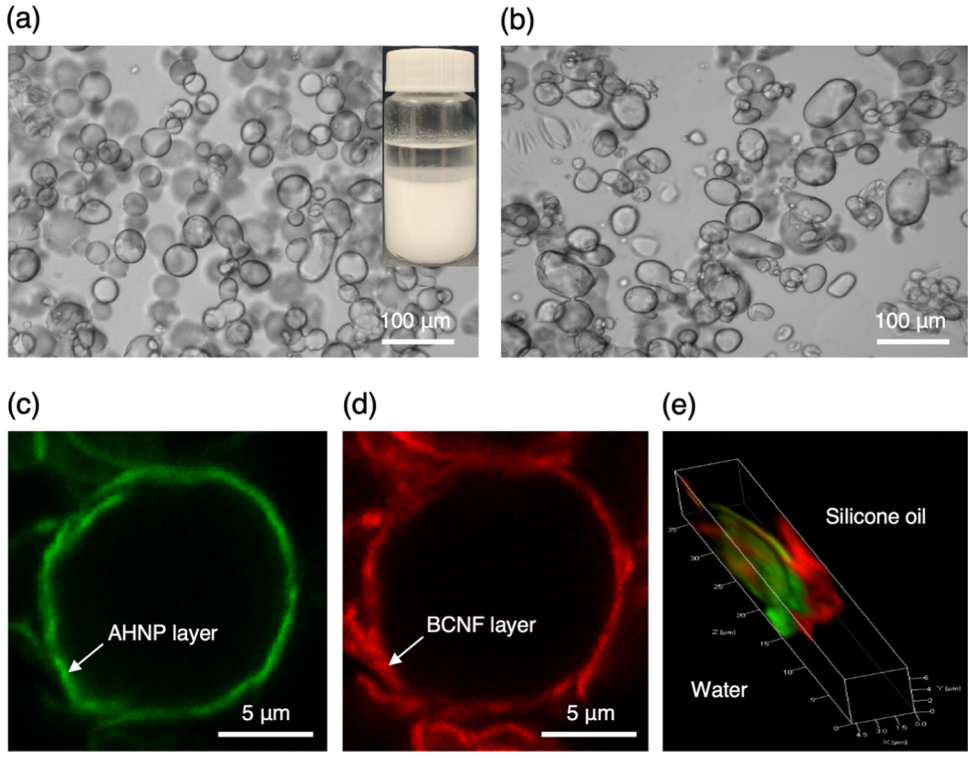


**Figure 4.** Bright-field microscopic images of the W/S Pickering emulsions stabilized with (a) the AHNPs only (b) a bilayer of the AHNPs and the BCNFs. The inset shows a vial image of the W/S emulsions with 0.15 wt % AHNPs. Visualization of an AHNP−BCNF-bilayered membrane structure at the W/S interface. CLSM images of (c) the AHNP layer and (d) the BCNF layer of the AHNP−BCNF-bilayered W/S emulsion drop. (e) *Z*-stack 3D CLSM image of the magnified outer interface and the inner interface of the AHNP−BCNF-bilayered W/S emulsion drop. For these observations, the emulsion was made using FITC-labeled AHNPs (green) and direct red 23-labeled BCNFs (red). The emulsions were prepared using 0.15 wt % AHNPs and 0.5 wt % BCNFs.

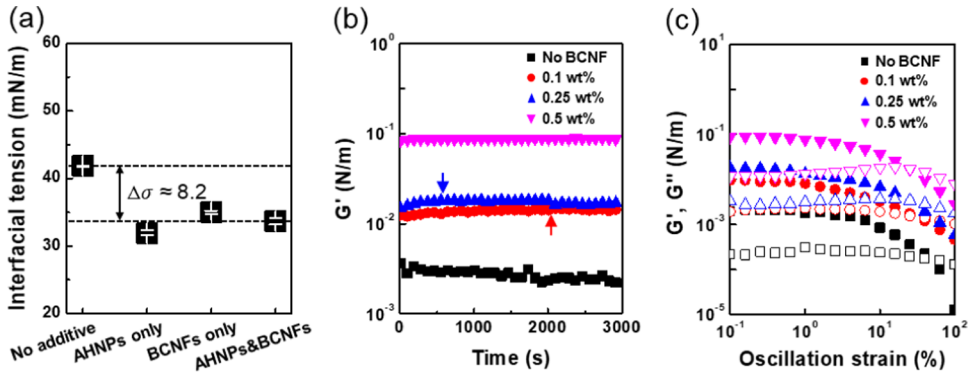


**Figure 5.** (a) Interfacial tension at the W/S interface in the presence of the AHNPs in silicone oil, BCNFs in water, and combined AHNPs and BCNFs in each phase. (b) Interfacial $G'$ vs oscillation time (arrow: plateau time) and (c) interfacial $G'$ (solid symbol) and $G''$ (open symbol) vs oscillation strain by increasing the BCNF concentration against a fixed AHNP concentration (0.15 wt %).

see the inset). BCNFs only could not emulsify silicone oil due to their high hydrophilicity. Interestingly, when BCNFs were used together with AHNPs, a stable Pickering emulsion was formed even at low AHNP concentrations, less than 1 wt %. Structurally stable W/S emulsions could be obtained within the phase inversion ratio (5:5, v/v). Since there was no phase separation or water elusion from the emulsion system, the percentage of emulsified water based on the total amount of water added to the systems reached 100%. Also, the uniform W/S emulsion with an average droplet size of ∼70 $\mu$m could be obtained at the ratio of interest, 3:7 (v/v) (Figure S2). The Pickering emulsion armored with the AHNPs and BCNFs exhibited a slightly nonspherical and polygonal shape compared to that stabilized with AHNPs only, which indicates that the AHNPs and BCNFs strongly adsorb to form a rigid layer at the interface (Figure 4b). To directly confirm which structure was formed at the W/S interface because of coacervation of the AHNPs and the BCNFs, CLSM observation was carried out for a W/S Pickering emulsion drop stabilized with the AHNPs labeled with FITC (green) and the direct red 23-labeled BCNFs (red) (Figure 4c,d). Since the coexistence of the AHNPs and BCNFs was detected at the interface, it was clear that they were the components of the coacervate. By analyzing the reconstructed three-dimensional (3D) CLSM image, we could observe that the AHNP layer faced the silicone oil phase and the BCNF layer faced the


https://doi.org/10.1021/acs.langmuir.0c03082
*Langmuir* 2021, 37, 3828−3835

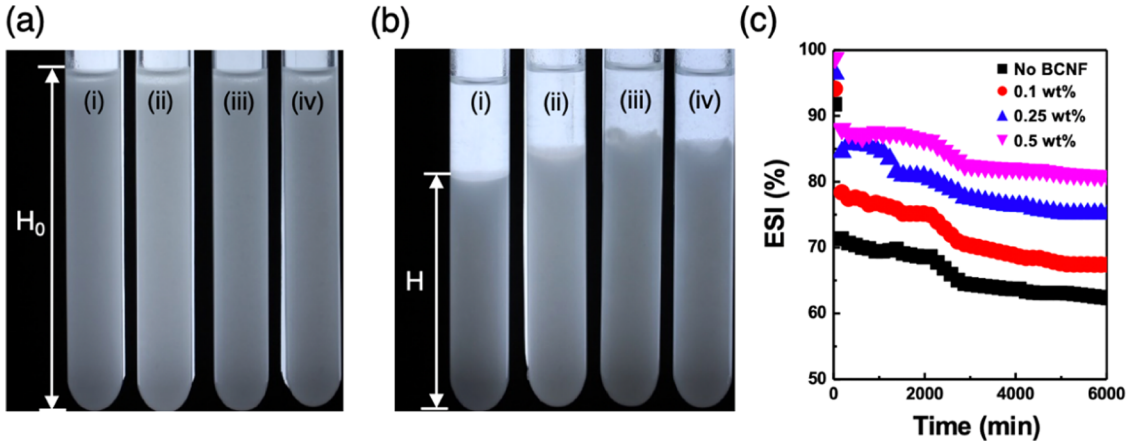


**Figure 6.** Sedimentation behaviors of the W/S Pickering emulsions prepared by varying the BCNF concentration against a fixed AHNP concentration (0.15 wt %): (i) no BCNF, (ii) 0.1 wt %, (iii) 0.25 wt %, and (iv) 0.5 wt % BCNFs. Actual images of the W/S Pickering emulsions loaded in test tubes (a) upon preparation and (b) after 96 h of sedimentation. (c) ESI against the storage time.

aqueous phase, thus directly verifying that the coacervate indeed has a bilayer structure (Figure 4e).

**Confirmation of Solid Interface Formation via Interfacial Rheological Measurements.** The addition of the AHNPs and the BCNFs in each dispersion phase slightly lowered the W/S interfacial tension by ~8.2 mN/m (Figure 5a). This indicates that neither of them was properly oriented at the interface. There was no significant change in the interfacial tension even when the AHNPs and the BCNFs were introduced together; however, they produced a stable W/S emulsion. This interesting result could be attributed to the fact that the AHNPs and the BCNFs formed an interface solely via interfacial solidification. To prove this, we conducted an interfacial rheological measurement on the W/S interfaces. In this rheology study, the silicone oil phase contained a fixed low concentration of the AHNPs (0.15 wt %) and the aqueous phase contained different concentrations of the BCNFs (to 0.5 wt %). The test of oscillation time sweep showed that the interfacial modulus of the AHNP−BCNF-coacervated interfaces reached a plateau with time, whereas the interfacial modulus of the interface with the AHNPs only gradually decreased. This is because of the lack of an effective association of the AHNPs with the interface (Figure 5b). Compared to the case of introducing AHNPs only, the interfacial moduli increased by 1 order of magnitude when BCNFs ranging between 0.1 and 0.25 wt % were introduced, thus supporting our proposal that they form a solid interface. In addition, the speed of coacervation, characterized by the time taken to reach a plateau (marked with an arrow in Figure 5b), decreased with the increase of the concentration of BCNFs. It means that the addition of BCNFs speeded up the formation of coacervate membranes. Notably, the interfacial modulus further increased by 1 order of magnitude when 0.5 wt % BCNFs were introduced. In our further investigation on the interfacial storage modulus ($G'$) and loss modulus ($G''$) as functions of the oscillation strain for the identical interfaces, $G'$ and $G''$ exhibited a similar pattern as the time-dependent interfacial moduli (Figure 5c). Based on these results, we infer that the introduction of excess BCNFs could induce a structural change to a solidified interface.

**Sedimentation Behaviors of W/S Pickering Emulsions.** To determine how interfacial coacervation of the AHNPs and the BCNFs affects the stability of the W/S interface, we performed a sedimentation test on the Pickering emulsions prepared according to the composition of the interface (Figure 6a,b). The sedimentation kinetics were quantitatively determined using the emulsion sedimentation index (ESI),[33,34] defined as ESI (%) $= \frac{H}{H_0} \times 100$ (%), where $H$ and $H_0$ are the heights of the sedimented and initial emulsion phase in the tube, respectively. Since the water dispersion phase ($\rho \sim 1$ g/mL) is heavier than the continuous phase of silicon oil ($\rho$ 0.89−0.87 g/mL), the sedimentation phenomenon was observed for all emulsions. In addition, as the composition ratio of the BCNFs against the AHNPs increased, the ESI increased from ~65 to ~85% during a test period of 4 days (Figure 6c). For the W/S Pickering emulsions prepared by increasing the AHNP concentration against a fixed BCNF concentration, a similar ESI increase trend was also observed (Figure S3). These results indicate that the formation of interfacial coacervates made of an AHNP−BCNF bilayer significantly improved the structural stability of the W/S Pickering emulsions.

**Theoretical Understanding of the Sedimentation Kinetics of the W/S Pickering Emulsions.** To verify how different interfacial properties could influence the phase separation behaviors of the W/S emulsions, the theoretically calculated sedimentation velocity was compared with that obtained experimentally. In this study, the Stokes equation was modified for a Pickering emulsion drop whose interface is made of nanoplatelet particles.[35] Thereafter, for a W/O Pickering emulsion system, the thickness of the assembled layer of nanoplatelets protruding into the oil phase ($h$) and the sum of the radius of the core droplet and half of the thickness of the nanoplatelets ($R^*$) can be expressed by $h = R_{np}(1 - \cos\theta)$ and $R^* = R_d\left(1 - \frac{R_{np}}{R_d}\cos\theta\right)$, respectively, where $R_{np}$ is the thickness of the nanoplatelets ($2h$), $\theta$ is the three-phase contact angle through the aqueous phase, and $R_d$ is the radius of the core droplet. Other parameters were adjusted based on references (see the Supporting Information). Finally, the modified Stokes equation for the W/O emulsion was obtained as $U_0 = \frac{2gR_{eff}^2(\rho_{d,eff} - \rho_S)}{9\mu}$, where $U_0$ is the sedimentation velocity of the emulsion, $R_{eff}$ ($=R_d + h$) is the effective radius of the droplet including platelet particles, $\mu$ is the viscosity of the emulsion, $\rho_{d,eff}$ is the effective density of the water droplet, and


https://doi.org/10.1021/acs.langmuir.0c03082
Langmuir 2021, 37, 3828−3835

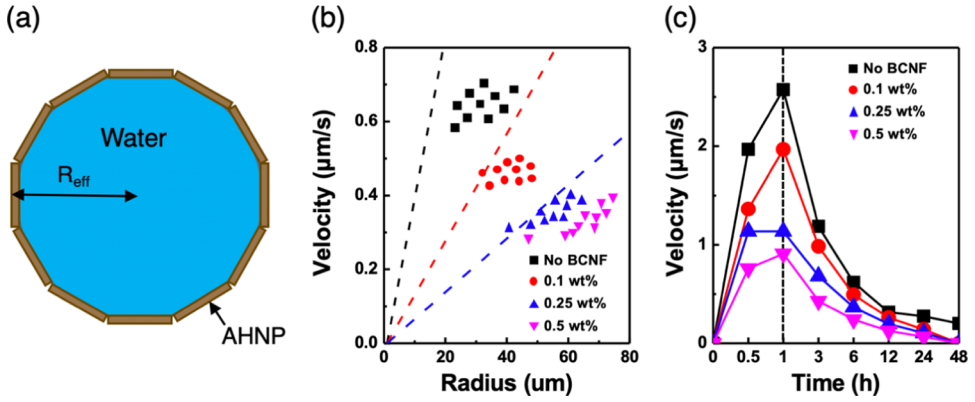


**Figure 7.** (a) Schematic illustration of a Pickering emulsion droplet for theoretical consideration. (b) Predicted sedimentation velocity of the Pickering emulsions from the modified Stokes equation. The dashed lines were determined at the emulsion viscosity of 500 Pa·s (black), 1500 Pa·s (red), and 3000 Pa·s (blue). (c) Actual sedimentation velocity of the Pickering emulsions prepared by varying the BCNF concentration against a fixed AHNP concentration (0.15 wt %).

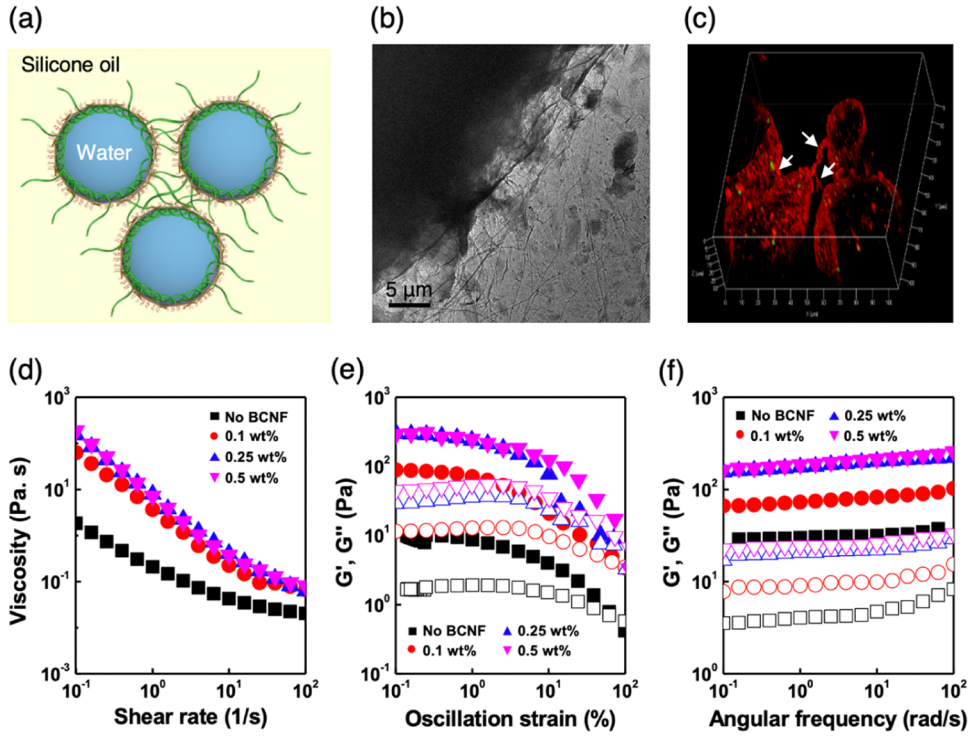


**Figure 8.** (a) Schematic illustration of the Pickering emulsion drops connected with the BCNF bridges. (b) Direct observation of the BCNF bridges at the periphery of a water drop via cryo-TEM analysis. (c) Z-stack 3D CLSM image showing a reconstructed 3D structure of Pickering emulsion drops connected with the BCNF bridges. (d) Viscosity vs shear rate, (e) $G'$ (solid symbol) and $G''$ (open symbol) vs oscillation strain, and (f) $G'$ (solid symbol) and $G''$ (open symbol) vs angular frequency of Pickering emulsions prepared by varying the BCNF concentration against a fixed AHNP concentration (0.15 wt %).

$\rho_s$ is the density of silicone oil. Based on the modified equation, the dependency of the sedimentation velocity on the drop size was fitted by varying the viscosity of the emulsions. Through the comparison with the sedimentation velocities calculated from the experimental parameters for given viscosities (Table S2), we could establish that the sedimentation velocity of the Pickering emulsions behaved according to the modified Stokes equation (Figure 7b). Further, we measured the sedimentation velocities of the Pickering emulsions with storage time (Figure 7c). The sedimentation velocity increased for 1 h and then gradually decreased, which is the common pattern of conventional emulsions. In addition, the sedimentation velocity at any given time was predominantly dependent on the concentration of the BCNF. Evidently, the sedimentation velocities of the Pickering emulsions with the bilayered coacervate gradually decreased to almost zero, which occurred much faster compared to the case of conventional emulsions. This indicates that the emulsion phase was clumped or hardened in any way during sedimentation.[36,37]

**Interconnection of the W/S Pickering Emulsion Drops via Fibrillary Bridging.** Such an unusual sedimentation behavior of the W/S emulsions with the bilayered coacervate could be attributed to the interconnection of drops through BCNF bridging, as illustrated in Figure 8a. From cryo-HAADF-STEM analysis and element mapping via electron-dispersive spectroscopy, we observed a bundle of BCNFs at the


https://doi.org/10.1021/acs.langmuir.0c03082
Langmuir 2021, 37, 3828−3835

periphery of a water drop (Figures 8b and S4a–d). The reconstructed 3D CLSM image clearly revealed that the emulsion droplets were connected by BCNF bridges (Figure 8c). In our emulsions system, the thermodynamic potential for the internal energy density increased when an excessive amount of the BCNFs was unfavorably located in the aqueous drop.[38] To meet the equilibrium of the interfacial entropy between the water and silicone oil phases, the diffusion transport for the extra BCNFs should occur through the interstitial imperfection points at the interface. In addition, the solvophilic effect presumably led to the intermolecular interaction between the extruded BCNFs from droplets in the silicone oil phase, which seemed to be the origin for the formation of a fibrillary network.[39,40] The interconnection of droplets via BCNF bridging led to significant changes in the rheological properties of the emulsions. The viscosity of the W/S emulsions with a BCNF–AHNP coacervate increased over 100-fold than that of the BCNF-free emulsion. Moreover, from the observation of $G'$ and $G''$ as functions of oscillation strain and angular frequency, we demonstrated that the W/S emulsions prepared via interfacial coacervation exhibited typical viscoelastic or solid-like behavior (Figure 8e,f). These rheology results elucidate that the BCNFs formed a physically associated fibrillary network in the W/S emulsion phase, which also explains why such extraordinary sedimentation kinetics occurred.

## CONCLUSIONS

In summary, we present a new type of W/S Pickering emulsion system whose interface is arranged with a bilayered coacervate. Successful fabrication of the bilayered coacervate structure was confirmed by direct visualization with *Z*-stack 3D CLSM. From the study of interfacial rheology, we established that the formation of interfacial coacervates made the interface mechanically robust. In particular, we showed that the interconnection of drops by BCNF bridging makes the emulsion phase viscoelastic or solid-like, thus leading to the production of the structurally stable Pickering emulsions. Based on these findings, we expect that the proposed bilayered coacervation technology will play a crucial role in the development of a highly promising Pickering emulsion system that directs future cosmetic and pharmaceutical formulations.

## ASSOCIATED CONTENT

### Supporting Information

The Supporting Information is available free of charge at https://pubs.acs.org/doi/10.1021/acs.langmuir.0c03082.

Detailed calculation of other requisites for the modified equation; fitting parameter values of the modified Stokes equation; phase separation kinetics of a Pickering emulsion at a high BCNF concentration; and cryo-HAADF-STEM image and element mappings of a Pickering emulsion armored with AHNPs and BCNFs (PDF)

## AUTHOR INFORMATION


### Corresponding Author

**Jin Woong Kim** − *School of Chemical Engineering, Sungkyunkwan University, Suwon 16419, Republic of Korea;* orcid.org/0000-0002-6485-9936; Phone: +82-290-7346; Email: jinwoongkim@skku.edu

### Authors

**Yeong Sik Cho** − *School of Chemical Engineering, Sungkyunkwan University, Suwon 16419, Republic of Korea*

**Sung Ho Lee** − *School of Chemical Engineering, Sungkyunkwan University, Suwon 16419, Republic of Korea; Sunjin Beauty Science Co., Ansan 15612, Republic of Korea*

**Hye Min Seo** − *School of Chemical Engineering, Sungkyunkwan University, Suwon 16419, Republic of Korea*

**Kyounghee Shin** − *School of Chemical Engineering, Sungkyunkwan University, Suwon 16419, Republic of Korea*

**Min Ho Kang** − *Center for Nanoparticle Research, Institute for Basic Science (IBS), Seoul 08826, Republic of Korea; School of Chemical and Biological Engineering and Institute of Chemical Processes, Seoul National University, Seoul 08826, Republic of Korea*

**Minyoung Lee** − *Center for Nanoparticle Research, Institute for Basic Science (IBS), Seoul 08826, Republic of Korea; School of Chemical and Biological Engineering and Institute of Chemical Processes, Seoul National University, Seoul 08826, Republic of Korea*

**Jungwon Park** − *Center for Nanoparticle Research, Institute for Basic Science (IBS), Seoul 08826, Republic of Korea; School of Chemical and Biological Engineering and Institute of Chemical Processes, Seoul National University, Seoul 08826, Republic of Korea;* orcid.org/0000-0003-2927-4331

Complete contact information is available at: https://pubs.acs.org/10.1021/acs.langmuir.0c03082


### Author Contributions

Y.S.C. and S.H.L. equally contributed to this work. Y.S.C., S.H.L., and J.W.K. conceived and designed the experiments. Y.S.C. and H.M.S. fabricated AHNPs and BCNFs. S.H.L. and J.W.K. designed and demonstrated theoretical calculations. M.L., M.H.K., and J.P. conducted cryo-HAADF-STEM observations, Y.S.C., K.S., and J.W.K. cowrote the paper. All authors discussed the results and commented on the manuscript.

### Notes

The authors declare no competing financial interest.

## ACKNOWLEDGMENTS

This study was supported by the National Research Foundation of Korea (NRF) grant funded by the Korean government (MSIT) (No. NRF-2019R1A2C1086383). J.P. acknowledges financial support for TEM analysis and characterization from the Institute for Basic Science (IBS-R006-D1); NRF was funded by the Korean government (MSIT) under Contract No. 2017R1A5 A1015365.

## REFERENCES

(1) Zhang, J.; Zhou, C. H.; Petit, S.; Zhang, H. Hectorite: Synthesis, modification, assembly and applications. *Appl. Clay Sci* **2019**, *177*, 114–138.

(2) Yu, D.; Li, G.; Liu, W.; Li, Y.; Song, Z.; Wang, H.; Guan, F.; Chen, X. A fluorescent pickering-emulsion stabilizer prepared using carbon nitride quantum dots and laponite nanoparticles. *Colloids Surf., A* **2019**, *563*, 310–317.

(3) Ganley, W. J.; van Duijneveldt, J. S. Controlling the Rheology of Montmorillonite Stabilized Oil-in-Water Emulsions. *Langmuir* **2017**, *33*, 1679–1686.

(4) Hong, J. S. Aggregation of hydrophilic/hydrophobic montmorillonites at oil–water interface. *Appl. Clay Sci.* **2016**, *119*, 257–265.

(5) Dai, H.; Wu, J.; Zhang, H.; Chen, Y.; Ma, L.; Huang, H.; Huang, Y.; Zhang, Y. Recent advances on cellulose nanocrystals for Pickering emulsions: Development and challenge. *Trends Food Sci. Technol.* **2020**, *102*, 16−29.
(6) Kim, H.; Cho, J.; Cho, J.; Park, B. J.; Kim, J. W. Magnetic-Patchy Janus Colloid Surfactants for Reversible Recovery of Pickering Emulsions. *ACS Appl. Mater. Interfaces* **2018**, *10*, 1408−1414.
(7) Dong, J.; Worthen, A. J.; Foster, L. M.; Chen, Y.; Cornell, K. A.; Bryant, S. L.; Truskett, T. M.; Bielawski, C. W.; Johnston, K. P. Modified montmorillonite clay microparticles for stable oil-in-seawater emulsions. *ACS Appl. Mater. Interfaces* **2014**, *6*, 11502−13.
(8) Xiang, F.; Tzeng, P.; Sawyer, J. S.; Regev, O.; Grunlan, J. C. Improving the gas barrier property of clay-polymer multilayer thin films using shorter deposition times. *ACS Appl. Mater. Interfaces* **2014**, *6*, 6040−8.
(9) Kim, J. E.; Yim, D.; Lee, C. H.; Jun, B.; Nam, J.; Han, S. H.; Lee, S. U.; Kim, J.-H.; Kim, J. W. Environmental Stimuli-Irresponsive Long-Term Radical Scavenging of 2D Transition Metal Dichalcogenides through Defect-Mediated Hydrogen Atom Transfer in Aqueous Media. *Adv. Funct. Mater.* **2018**, *28*, No. 1802737.
(10) Qiao, X. G.; Dugas, P. Y.; Prevot, V.; Bourgeat-Lami, E. Surfactant-free synthesis of layered double hydroxide-armored latex particles. *Polym. Chem.* **2020**, *11*, 3195−3208.
(11) Inam, M.; Jones, J. R.; Perez-Madrigal, M. M.; Arno, M. C.; Dove, A. P.; O'Reilly, R. K. Controlling the Size of Two-Dimensional Polymer Platelets for Water-in-Water Emulsifiers. *ACS Cent. Sci.* **2018**, *4*, 63−70.
(12) Wang, Z.; Gao, S.; Liu, X.; Tian, Y.; Wu, M.; Niu, Z. Programming Self-Assembly of Tobacco Mosaic Virus Coat Proteins at Pickering Emulsion Interfaces for Nanorod-Constructed Capsules. *ACS Appl. Mater. Interfaces* **2017**, *9*, 27383−27389.
(13) Song, Y.; Hagen, D. A.; Qin, S.; Holder, K. M.; Falke, K.; Grunlan, J. C. Edge Charge Neutralization of Clay for Improved Oxygen Gas Barrier in Multilayer Nanobrick Wall Thin Films. *ACS Appl. Mater. Interfaces* **2016**, *8*, 34784−34790.
(14) Shin, J.-h.; Park, J.-w.; Kim, H.-j. Clay-polystyrene nanocomposite from pickering emulsion polymerization stabilized by vinylsilane-functionalized montmorillonite platelets. *Appl. Clay Sci.* **2019**, *182*, No. 105288.
(15) Zhang, L.; Li, Z.; Wang, L.; Sun, D. High temperature stable W/O emulsions prepared with in-situ hydrophobically modified rodlike sepiolite. *J. Colloid Interface Sci.* **2017**, *493*, 378−384.
(16) Liang, S.; Li, C.; Dai, L.; Tang, Q.; Cai, X.; Zhen, B.; Xie, X.; Wang, L. Selective modification of kaolinite with vinyltrimethoxysilane for stabilization of Pickering emulsions. *Appl. Clay Sci.* **2018**, *161*, 282−289.
(17) Yu, D.; Lin, Z.; Li, Y. Octadecenylsuccinic anhydride pickering emulsion stabilized by γ-methacryloxy propyl trimethoxysilane grafted montmorillonite. *Colloids Surf., A* **2013**, *422*, 100−109.
(18) Saari, H.; Johansson, D. B.; Knopp, N.; Sjöö, M.; Rayner, M.; Wahlgren, M. Pickering emulsions based on CaCl2-gelatinized oat starch. *Food Hydrocolloids* **2018**, *82*, 288−295.
(19) Sufi-Maragheh, P.; Nikfarjam, N.; Deng, Y.; Taheri-Qazvini, N. Pickering emulsion stabilized by amphiphilic pH-sensitive starch nanoparticles as therapeutic containers. *Colloids Surf., B* **2019**, *181*, 244−251.
(20) Wu, J.; Shi, M.; Li, W.; Zhao, L.; Wang, Z.; Yan, X.; Norde, W.; Li, Y. Pickering emulsions stabilized by whey protein nanoparticles prepared by thermal cross-linking. *Colloids Surf., B* **2015**, *127*, 96−104.
(21) Bell, R. V.; Parkins, C. C.; Young, R. A.; Preuss, C. M.; Stevens, M. M.; Bon, S. A. F. Assembly of emulsion droplets into fibers by microfluidic wet spinning. *J. Mater. Chem. A* **2016**, *4*, 813−818.
(22) Wang, J.; Deng, H.; Sun, Y.; Yang, C. Montmorillonite and alginate co-stabilized biocompatible Pickering emulsions with multiple-stimulus tunable rheology. *J. Colloid Interface Sci.* **2020**, *562*, 529−539.
(23) Shen, X.; Svensson Bonde, J.; Kamra, T.; Bulow, L.; Leo, J. C.; Linke, D.; Ye, L. Bacterial imprinting at Pickering emulsion interfaces. *Angew. Chem., Int. Ed.* **2014**, *53*, 10687−90.
(24) Lee, Y. R.; Park, D.; Choi, S. K.; Kim, M.; Baek, H. S.; Nam, J.; Chung, C. B.; Osuji, C. O.; Kim, J. W. Smart Cellulose Nanofluids Produced by Tunable Hydrophobic Association of Polymer-Grafted Cellulose Nanocrystals. *ACS Appl. Mater. Interfaces* **2017**, *9*, 31095−31101.
(25) Jimenez-Saelices, C.; Seantier, B.; Grohens, Y.; Capron, I. Thermal Superinsulating Materials Made from Nanofibrillated Cellulose-Stabilized Pickering Emulsions. *ACS Appl. Mater. Interfaces* **2018**, *10*, 16193−16202.
(26) Li, Y.; Liu, X.; Zhang, Z.; Zhao, S.; Tian, G.; Zheng, J.; Wang, D.; Shi, S.; Russell, T. P. Adaptive Structured Pickering Emulsions and Porous Materials Based on Cellulose Nanocrystal Surfactants. *Angew. Chem., Int. Ed.* **2018**, *57*, 13560−13564.
(27) Kim, D.; Lee, S.; Park, D.; Cho, Y. S.; Choi, S.; Nam, Y. S.; Kim, J. W. Fabrication of attractive hectorite nanoplatelets by high-pressure homogenization for shear-responsive reversible rheology modification of organogels. *J. Ind. Eng. Chem.* **2020**, *90*, 274−280.
(28) Ozdemir, O.; Armagan, B.; Turan, M.; Çelik, M. S. Comparison of the adsorption characteristics of azo-reactive dyes on mezoporous minerals. *Dyes Pigm.* **2004**, *62*, 49−60.
(29) Karataş, D.; Senol Arslan, D.; Kursun Unver, I.; Ozdemir, O. Coating Mechanism of AuNPs onto Sepiolite by Experimental Research and MD Simulation. *Coatings* **2019**, *9*, No. 785.
(30) Das, A.; Thakur, A. K. Effect of organomodifier on the electrical property of a smectite clay Hectorite. *Mater. Today: Proc.* **2020**, *28*, 124−126.
(31) Joshi, G. V.; Kevadiya, B. D.; Patel, H. A.; Bajaj, H. C.; Jasra, R. V. Montmorillonite as a drug delivery system: intercalation and in vitro release of timolol maleate. *Int. J. Pharm.* **2009**, *374*, 53−57.
(32) Gadige, P.; Bandyopadhyay, R. Electric field induced gelation in aqueous nanoclay suspensions. *Soft Matter* **2018**, *14*, 6974−6982.
(33) Joshi, D.; Bargteil, D.; Caciagli, A.; Burelbach, J.; Xing, Z.; Nunes, A. S.; Pinto, D. E.; Araújo, N. A.; Brujic, J.; Eiser, E. Kinetic control of the coverage of oil droplets by DNA-functionalized colloids. *Sci. Adv.* **2016**, *2*, No. e1600881.
(34) Shao, W.; Pan, X.; Liu, X.; Teng, F.; Yuan, S. Microencapsulation of Algal Oil Using Spray Drying Technology. *Food Technol. Biotechnol.* **2018**, *56*, 65−70.
(35) Pal, R. Modeling of Sedimentation and Creaming in Suspensions and Pickering Emulsions. *Fluids* **2019**, *4*, No. 186.
(36) Jia, H.; Wu, H.; Wei, X.; Han, Y.; Wang, Q.; Song, J.; Dai, J.; Yan, H.; Liu, D. Investigation on the effects of AlOOH nanoparticles on sodium dodecylbenzenesulfonate stabilized o/w emulsion stability for EOR. *Colloids Surf., A* **2020**, *603*, No. 125278.
(37) Zembyla, M.; Lazidis, A.; Murray, B. S.; Sarkar, A. Water-in-Oil Pickering Emulsions Stabilized by Synergistic Particle-Particle Interactions. *Langmuir* **2019**, *35*, 13078−13089.
(38) Sharma, A.; Nehra, S. P.; Vijay, Y. K.; Jain, I. P. Fast mass and charge transport through electrically aligned CNT/polymer nanocomposite membranes. *Int. J. Energy Res.* **2016**, *40*, 770−775.
(39) Yang, L.; Adam, C.; Nichol, G. S.; Cockroft, S. L. How Much Do van der Waals Dispersion Forces Contribute to Molecular Recognition in Solution. *Nat. Chem.* **2013**, *5*, 1006−1010.
(40) Vangara, R.; van Swol, F.; Petsev, D. N. Solvophilic and solvophobic surfaces and non-Coulombic surface interactions in charge regulating electric double layers. *J. Chem. Phys.* **2018**, *148*, No. 044702.


https://doi.org/10.1021/acs.langmuir.0c03082
*Langmuir* 2021, 37, 3828−3835